SUPPORTING INFORMATION

Manuscript Title: **The nanocrystalline structure of basaluminite, an aluminum hydroxide sulfate from acid mine drainage.**

Authors:

Sergio Carrero*: Department of Earth Science, University of Huelva, Campus 'El Carmen', 21071, Huelva, Spain.

Alejandro Fernandez-Martinez: CNRS, ISTerre, F-38041 Grenoble, France; Université Grenoble Alpes, ISTerre, F-38041 Grenoble, France.

Rafael Pérez-López: Department of Earth Science, University of Huelva, Campus 'El Carmen', 21071, Huelva, Spain.

Daniel Lee: Université Grenoble Alpes, INAC, F-38000 Grenoble, France. CEA, INAC, F-38000 Grenoble, France.

Giuliana Aquilanti: Elettra-Sincrotrone Trieste, s.s. 14 km 165.3, 34149 Basovizza. Trieste, Italy.

Agnieszka Poulain: ESRF, The European Synchrotron, 71 Avenue des Martyrs, Grenoble, 38000, France.

Alba Lozano: Institute of Environmental Assessment and Water Research (IDAEA-CSIC). Jordi Girona 18, 08034 Barcelona, Spain.

José Miguel Nieto: Department of Earth Science, University of Huelva, Campus 'El Carmen', 21071, Huelva, Spain.

*corresponding author email: sergio.carrero@dgeo.uhu.es

S1 Details on partial Pair Distribution Function

The partial PDFs of felsöbányaite were calculated using the PDFGui software (Farrow et al., 2009) in order to ascertain what are the atomic pairs that contribute more to the total PDF. This allows simplifying the RMC simulation boxes by not including the atoms with atomic correlations with low weight factors, *i.e.*, those whose correlations are not well represented in the data. Partial PDFs between atoms *i* and *j* are weighted in the total PDF with a weight factor, $w_{ij}(r)$ (Egami and Billinge 2003):

$$w_{ij} = c_i c_j \frac{f_i f_j}{\langle f \rangle^2} \quad \text{Eq. S1}$$

where c_i and c_j are the concentrations of elements *i* and *j*, f_i and f_j their atomic form factors evaluated at Q = 0, and

$$\langle f \rangle^2 = (\Sigma_i c_i f_i)^2 \quad \text{Eq. S2}$$

S2 Details on Reverse Monte Carlo simulation

Three different starting structures were used in the Reverse Monte Carlo (RMC). All of them were built from the previously Rietveld refined felsöbányaite structure, which was modified in some cases by adding Al vacancies or SO_4^{2-} molecules to the structure to match the measured Al/S ratio from the PDF. These structures were: (i) a modified-felsöbányaite with the nominal Al/S = 4 (*fels1*); (ii) a modified-felsöbányaite including Al vacancies to reach an Al/S = 2.7 (*fels2*); and (iii) a modified-felsöbányaite including extra sulfate groups to reach Al/S = 2.7 (*fels3*). In the structure containing Al vacancies (*fels2*), all aluminum sites were fully coordinated by oxygen atoms. Different supercells were used in the refinements with sizes 1×1×1, 2×2×2 and 3×3×3. RMC modeling (McGreevy and Pusztail 1988; Keen 1998) was performed using the RMCprofile software (Tucker et al., 2014).

List of Tables:

Table S1. Felsöbányaite structural parameters obtained by Rietveld analysis.

Felsöbányaite	a (Å)	b (Å)	b (Å)	β(º)	V(Å^3)	U	V	W	X	U_{al}(Å^2)	U_O(Å^2)	U_S(Å^2)	d(Å)	σ_q(Å^{-1})	R_w(%)
P21-C22	12.968	9.9363	11.026	105.14	1166.0	-0.2168	-0.2587	0.0461	0.8784	0.0052	0.0176	0.0003	44.677	0.0978	19.43

Table S2. Close-contact distances used in the RMC runs for the different structures.

Pair	**O-O**	**O-Al**	**O-S**	**Al-Al**	**Al-S**	**S-S**
Distance	1.3	1.75	1.4	2.7	2.9	2.2

Table S3. Chemical results of solid samples.

	Natural bas.			Synthetic bas.		
	mg L^{-1}	**mmol g^{-1}**	**ratio**	**mg L^{-1}**	**mmol g^{-1}**	**ratio**
Al	200.29	7.31	4.00	219.48	8.20	4.00
S	83.18	2.55	1.40	96.99	3.05	1.49
Ca	1.35	0.03	0.02	0.43	0.01	0.01
Mg	0.07	0.03	0.02	0.01	0.01	0.00
Na	0.53	0.02	0.01	0.242	0.01	0.01
Fe	36.09	0.63	0.34	0.462	0.01	0.01
As	0.77	0.01	0.01	-0.3	-	-
Si	0.44	0.02	0.01	-0.044	-	-
OH	290.40	16.82	9.20	311.7	16.04	9.02
H2O	159.50	8.712	4.77	166.85	8.71	4.56
	$Al_4(OH)_{9.2}(SO_4)_{1.4}-4.77H_2O$			$Al_4(OH)_{9.02}(SO_4)_{1.49}-4.56H_2O$		

Table S4. Modeling parameters for S K-edge EXAFS in natural basaluminite with 1) 100% outer-sphere ligand, 2) 100%, and 3) 50% bidentate binucleate inner-sphere ligand.

Model	**Neighbor**	**N**	**σ^2**	**R**	**ΔE_0**	**V**	**$\Delta\chi^2$**
1*	One shell	5.119 ± 0.051	0.0004 ± 0.0002	1.453 ± 0.002	0.213 ± 1.320	4	16.3
2	Shell 1	5.172 ± 00783	0.0004 ± 0.0003	1.454 ± 0.003	0.354 ± 1.736	4	32.0
	Shell 2	2.000 (fixed)	0.0009 (fixed)	3.119 ± 0.029	0.354 ± 1.736		
3	Shell 1	5.208 ± 0.083	0.0003 ± 0.0003	1.453 ± 0.004	1.453 ± 1.771	4	33.3
	Shell 2	1.000 (fixed)	0.0009 (fixed)	2.109 ± 0.023	1.453 ± 1.771		

*best fit according to F-test.
V: nº of variable

Table S5. Modeling parameters for S K-edge EXAFS in synthetic basaluminite with 1) 100% outer-sphere ligand, 2) 100%, and 3) 50% bidentate binucleate inner-sphere ligand.

Model	**Neighbor**	**N**	**σ^2**	**R**	**ΔE_0**	**V**	**$\Delta\chi^2$**
1	One shell	4.023 ± 0.057	0.0003 ± 0.0003	1.459 ± 0.002	3.022 ± 1.402	3	36.0
2*	Shell 1	4.583 ± 0.051	0.0009 ± 0.0003	1.458 ± 0.003	2.049 ± 1.201	5	17.9
	Shell 2	2.000 (fixed)	0.0057 ± 0.0037	3.017 ± 0.033	2.049 ± 1.201		
3	Shell 1	4.532 ± 0.057	0.0009 ± 0.0003	1.458 ± 0.003	2.323 ± 1.350	5	21.8
	Shell 2	1 (fixed)	0.0091 ± 0.0069	2.188 ± 0.057	2.323 ± 1.350		

*best fit according to F-test.
V: nº of variable

Table S6. Fit parameters obtained from the different structural models compared with S k-edge EXAFS results in natural and synthetic basaluminites.

	Fit	Coordination 1	Proportion (%)	χ^2	R-factor	Ind. Point	Variable	Ind. Varible	Red. χ^2	Model 1	Model 2	F-test	Probability (%)
Bas-Nat	1	b. b. inner sp.	100	30.98	0.019	9.346	4	5.346	5.795	Fit 3	Fit 1	1.901	73.00
	2	b. m. inner sp.	100	33.28	0.020	9.346	4	5.346	6.226	Fit 3	Fit 2	2.043	75.00
	4	outer sp.	100	16.29	0.010	9.346	4	5.346	3.048				
Bas-Syn	1	b. b. inner sp.	100	17.87	0.008	9.346	5	4.346	4.112	Fit 1	Fit 2	2.206	79.00
	2	b. m. inner sp.	100	21.83	0.011	9.346	5	4.346	5.024	Fit 1	Fit 3	1.222	60.00
	4	outer sp.	100	36.01	0.017	9.346	3	6.346	5.674				

b.b. inner sp.: bidentate binucleate inner-sphere

b.m. inner sp.: bidentate mononucleate inner-sphere

outer sp.: outer-sphere

List of Figures:

Figure S1. Diffraction patter of natural felsöbányaite (red) and theoretical felsöbányaite (black) refine by Rietveld analysis from the structure proposed by Farkas & Pertlik (1997).

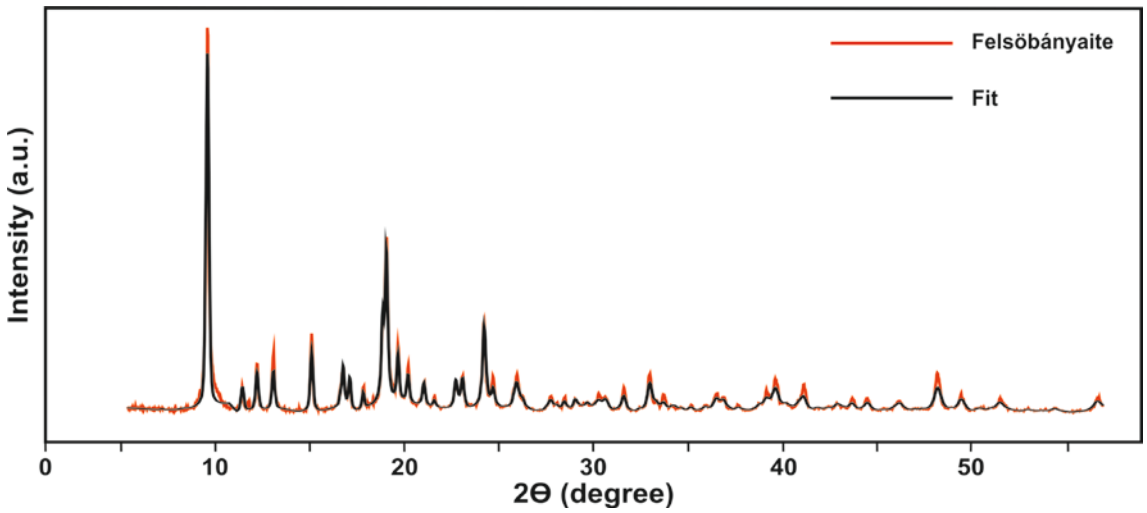

Figure S2. Thermo-gravimetric spectra of (a) felsöbányaite (black) and (b) natural (red) and (c) synthetic (blue) basaluminite. The shaded regions represent the different dehydration steps in felsöbányaite.

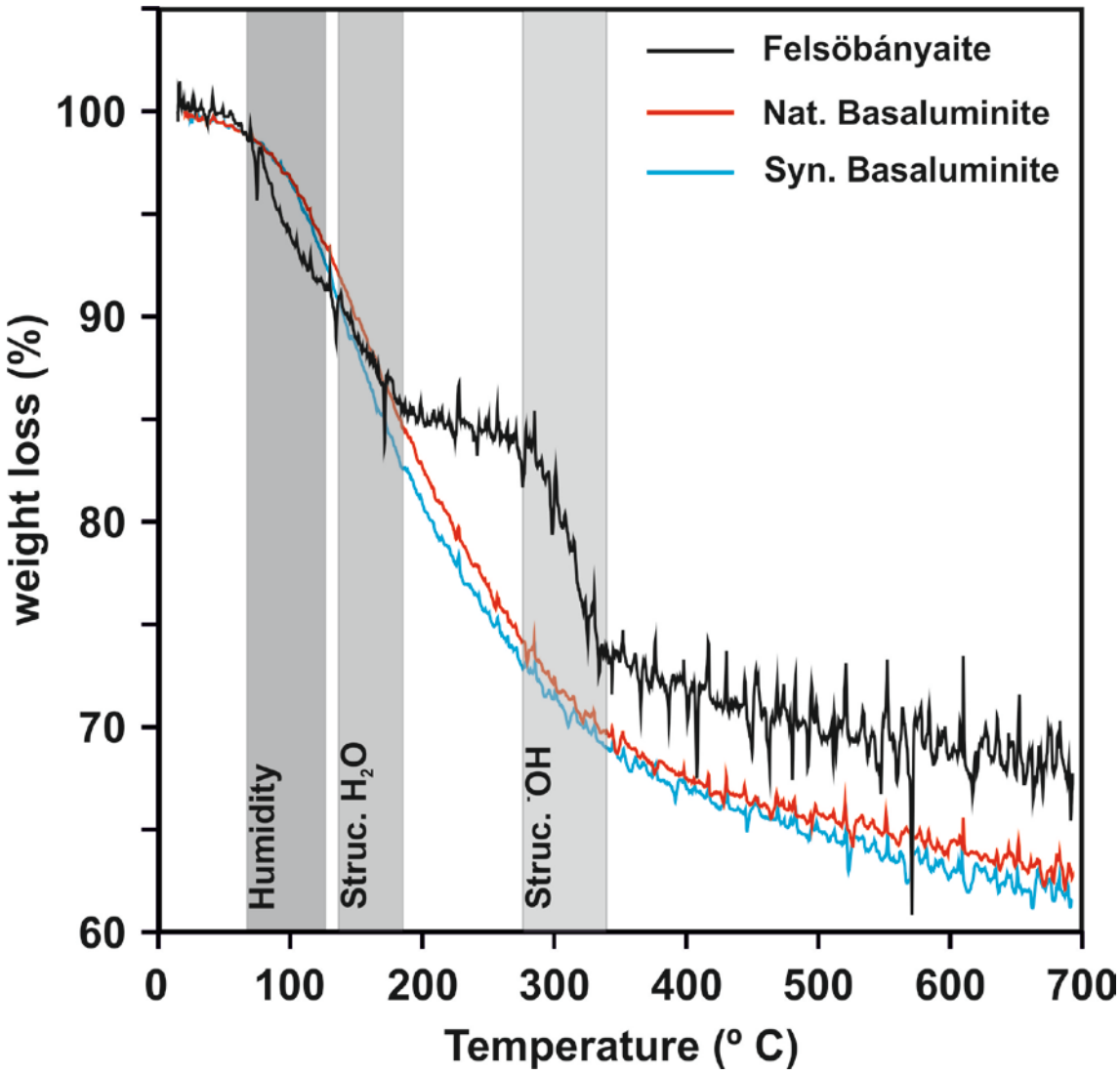

Figure S3. Basaluminite and felsöbányaite diffraction pattern. The patterns were collected using Cu kα_1 ($\lambda_{k\alpha1}$ = 1.5406 Å) and kα_2 ($\lambda_{k\alpha2}$ = 1.5444 Å) radiation in the range 2θ = 0-60°.

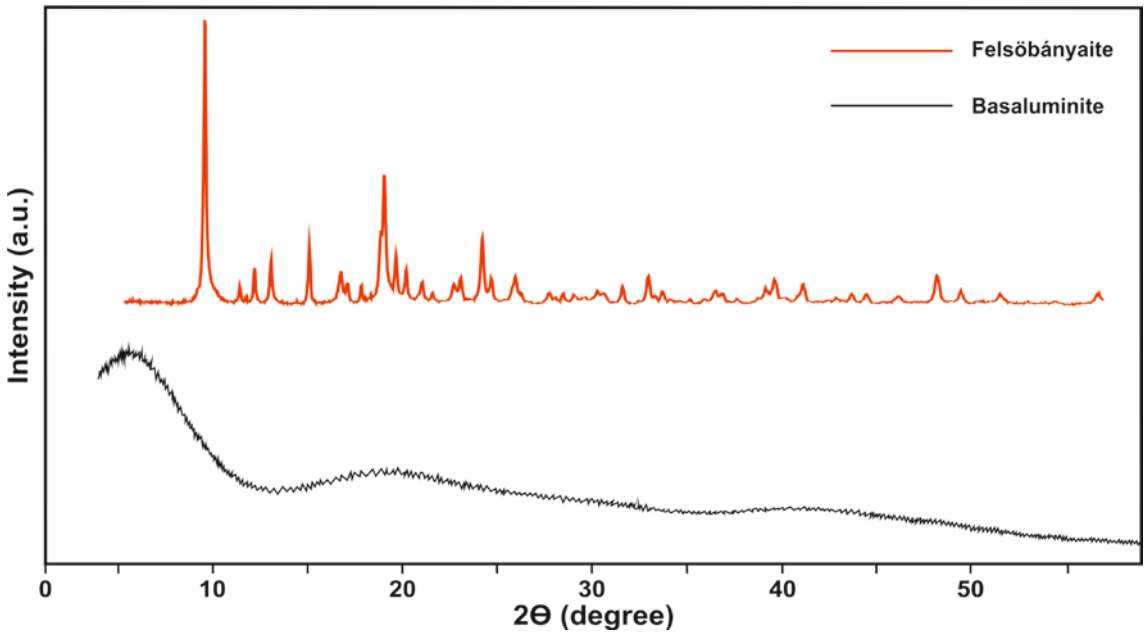

Figure S4. PDF of natural felsöbányaite (black), and calculated partial PDFs of felsöbányaite from the structure proposed by Farkas and Pertlik (1997) (grayscale).

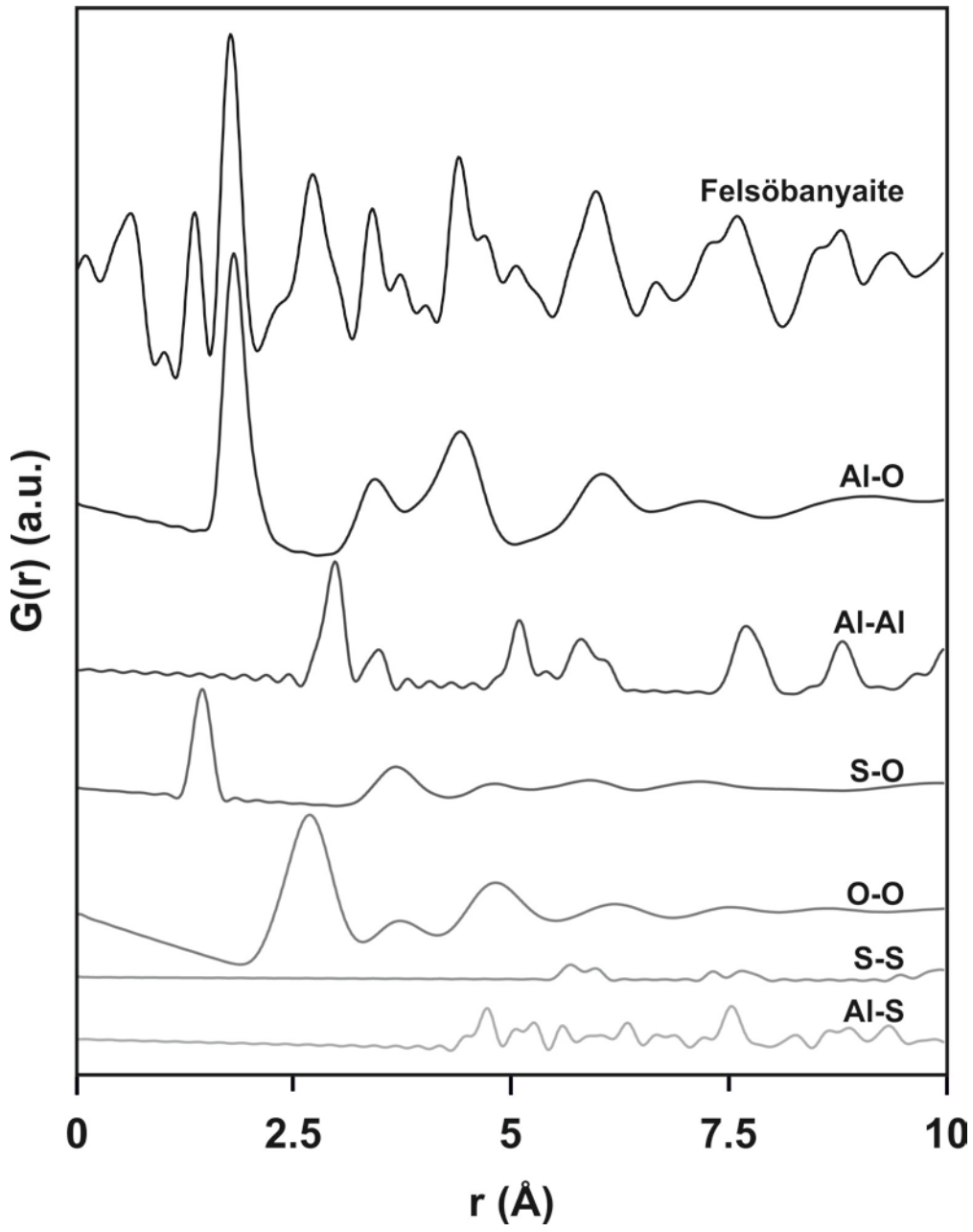

Figure S5. χ^2 evolution during RMC runs of *fels1[2,2,2]*, *fels2[2,2,2]* and *fels3[2,2,2]* supercells.

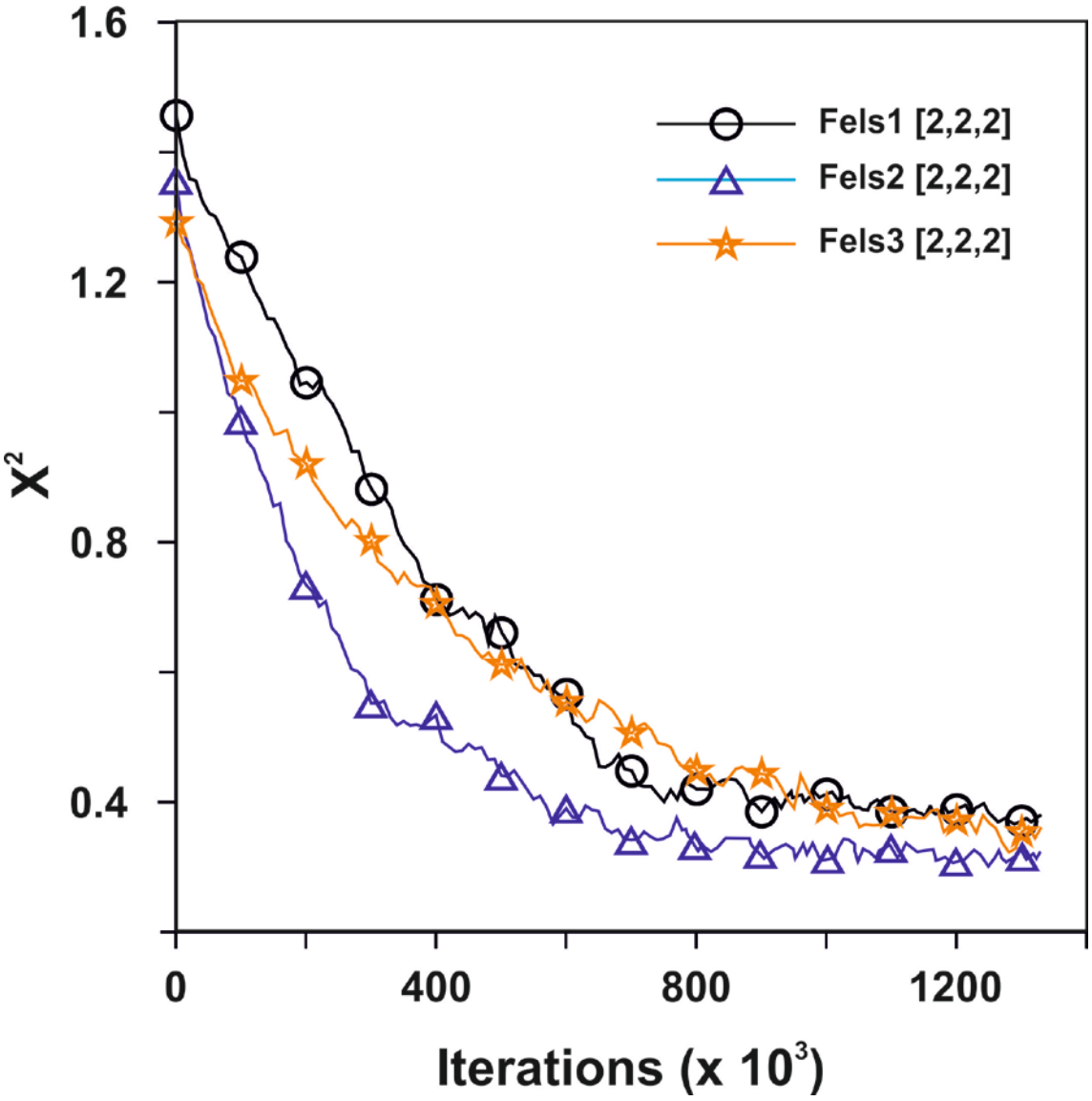

Figure S6. Different views of the final basaluminite structure, from (a) plane a-c, (b) plane a-b, and (c) b-edge of the *fels2 [2,2,2]* structural model after RMC refinement. The sections (a) and (c) reveal the octahedral-layer deformation and (b) shows the vacancies in Al-octahedral position imposed previously to RMC model by reach [Al]/[S] proportion in natural samples.

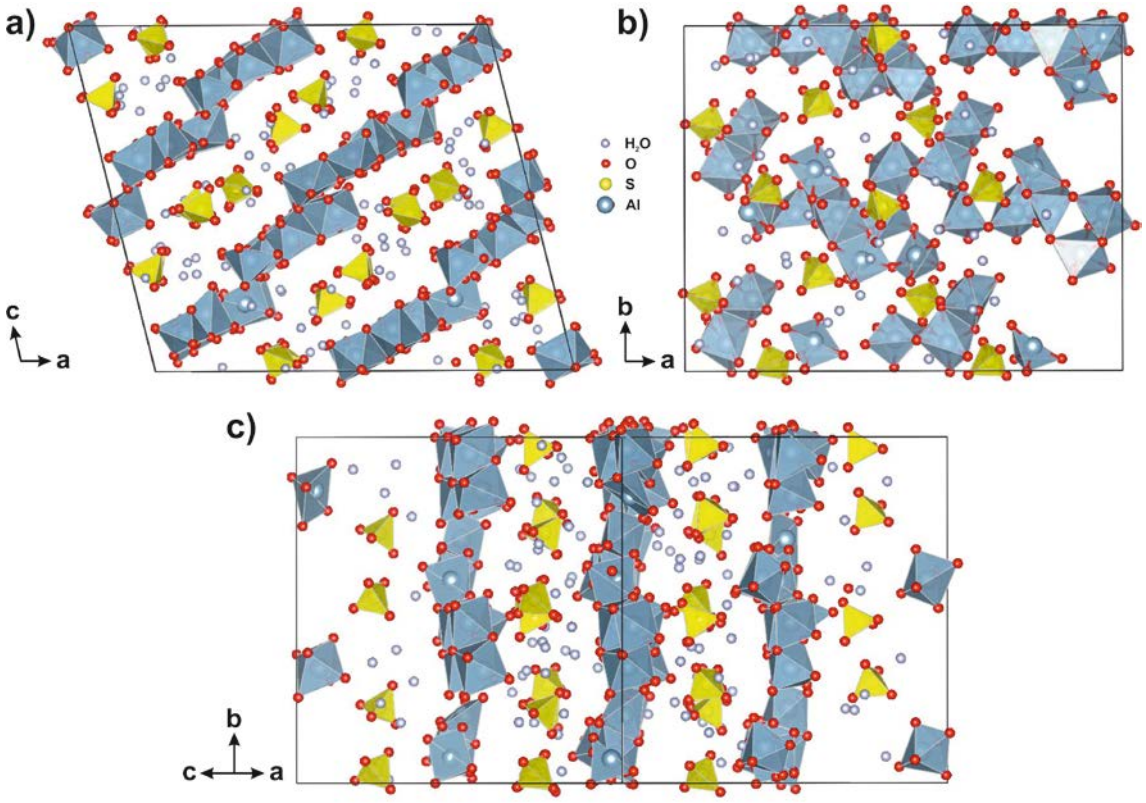

Figure S7: Al-O partial pair distribution function of a Rierveld refined felsöbányaite (black and the fels2[2,2,2] RMCrefined structure (red). The vertical lines indicate the Al-O distance for Al(IV), Al(V) and Al(VI).

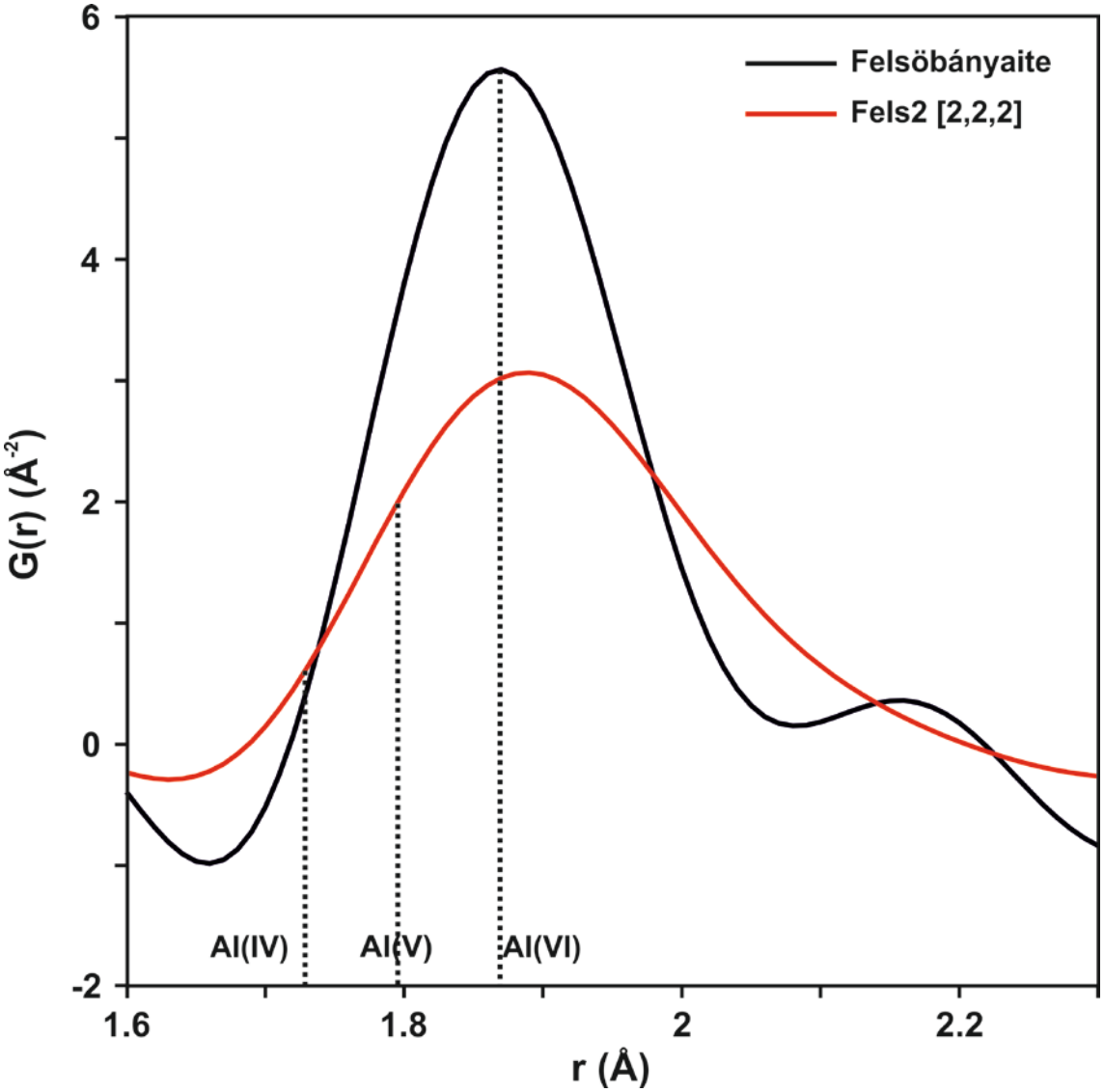

References

Egami, T., and Billinge, S.J.L. (2003) Underneath the Bragg Peaks: Structural analysis of complex materials. In Pergamon Material Series, Elsevier, Amsterdam.

Farkas, L., and Pertlik, F. (1997) Crystal structure determinations of felsöbányaite and basaluminite, Al4(SO4)(OH)10·4H2O. Acta Mineralogica-Petrographica, Szeged, 38, 5–15.

Farrow, C.L., Juhás, P., Liu, J.W., Bryndin, D., Bozin, E.S., Bloch, J., Proffen, T., and Billinge, S.J.L. (2009) PDFgui user guide.

Juhás, P., Davis, T., Farrow, C.L., and Billinge, S.J.L. (2013) PDFgetX3: A rapid and highly automatable program for processing powder diffraction data into total scattering pair distribution functions. Journal of Applied Crystallography, 46, 560–566.

Keen, D.A. (1998) Dynamic light scattering - applications of photon correlation spectroscopy. In Local Structure from Diffraction p. 101.

McGreevy, R.L., and Pusztail, L. (1988) Reverse Monte Carlo simulation: A new technique for the determination of dosodered structures. Molecular simulation, 1, 357–367.

Tucker, M., Dove, M., Goodwin, A., Keen, D.A., and Playford, H. (2014) RMCProfile User Manual. Code version 6.5.2, 0-155 p.